J|A|C|S COMMUNICATIONS

Published on Web 06/28/2010

Reducing the Symmetry of Bimetallic Au@Ag Nanoparticles by Exploiting Eccentric Polymer Shells

Shuangxi Xing,[†,‡] Yuhua Feng,[†] Yee Yan Tay,[§] Tao Chen,[†] Jun Xu,[†] Ming Pan,[†] Jiating He,[†] Huey Hoon Hng,[§] Qingyu Yan,[§] and Hongyu Chen*[,†]

Division of Chemistry and Biological Chemistry and School of Materials Science and Engineering, Nanyang Technological University, Singapore 637371, and Faculty of Chemistry, Northeast Normal University, Changchun, P. R. China

Received March 28, 2010; E-mail: hongyuchen@ntu.edu.sg

Abstract: We demonstrate a facile colloidal method for synthesizing Janus nanoparticles, whose eccentric polymer shells are exploited to fabricate eccentric bimetallic cores.

The synthesis of nanoparticles (NPs) has made tremendous advances in the past decades, particularly with respect to controlling crystal facets and achieving various basic shapes such as spheres, rods, and cubes.[1] However, it is unlikely that a sophisticated future nanodevice would be made only of such highly symmetrical NPs. Hence, breaking the symmetry of NPs is of paramount significance for developing assembling strategies and exploring novel properties.[1a,c,2] Janus NPs, named after the double-faced Roman god because of their diametric surface functionalities, represent a first and fundamental step in this direction. While syntheses of large (>100 nm) Janus particles have been well-established,[3] Janus NPs of smaller size present a greater challenge. A common synthetic theme is to utilize a surface, such as a liquid−liquid or liquid−solid interface, to expose the two sides of a particle to different chemical environments.[4] This allows selectivity in modifying only a portion of the particle surface. A different approach involves growing polymer[5] or inorganic materials[6] eccentrically on NPs, exploiting either nonwetting or lattice mismatch between the core and shell materials.

Most recently, there has been a growing interest in bimetallic core−shell NPs because of their unique optical and catalytic properties.[7] In particular, epitaxial overgrowth of a second metal on faceted metallic seeds has led to powerful control of heteronanocrystals with respect to both shape and metallic interfaces.[8] While lattice mismatch and certain reducing/capping agents, among others, are known to cause anisotropic overgrowth, methods for reducing the symmetry of bimetallic NPs are still very limited.[8e,9] During a typical colloidal synthesis, the second metal is isotropically available to the metallic seeds, and hence, it hinges upon the fine control of the metal(1)−metal(2) or metal(1)−ligand−metal(2) interfacial energy to manipulate the growth mode.

Here we report a new route for reducing the symmetry of bimetallic NPs by limiting the availability of the Ag being deposited on Au seeds via eccentric polymer shells. Previously, concentric triple-layer NPs, (Au@Ag)@PPy (PPy = polypyrrole), have been synthesized.[10a] The complex structure was formed as the uniform polymer shells guided isotropic Ag growth on Au seeds. We have now modified the synthesis to generate NPs with reduced symmetry,

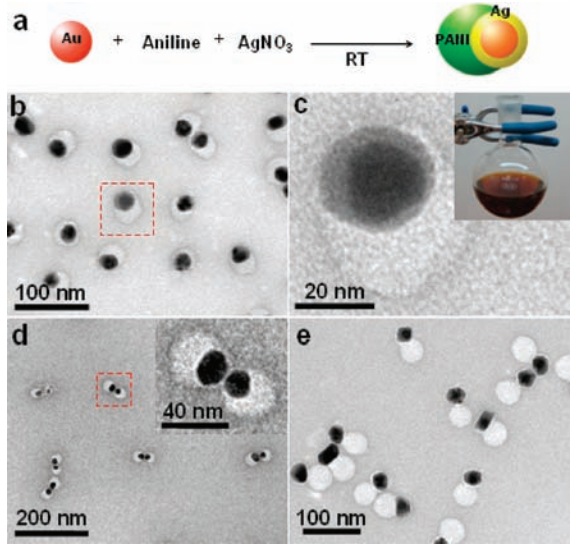

Figure 1. (a) Schematic illustration of the one-step colloidal synthesis of Janus NPs using Au NPs as seeds. (b, c) TEM images of *ecc*-(*con*-Au@Ag)-@PANI NPs at low and high magnification, respectively; the PANI shells appeared white in contrast to the stained background. (d) Dimers of *ecc*-(*con*-Au@Ag)@PANI formed during the drying process in the presence of stain solution. (e) TEM image of *ecc*-(*con*-Au@Ag)@PANI NPs as shown in (b) after incubation in an SDS solution (4 mM) overnight.

ecc-(*con*-Au@Ag)@PANI (PANI = polyaniline), where the bimetallic Au@Ag cores are concentric (*con*) whereas the PANI shells are eccentric (*ecc*). Utilizing the partial polymer shell to control the epitaxial overgrowth of Ag on the different sides of Au nanorods affords eccentric Au@Ag cores in a one-pot reaction.

To prepare the *ecc*-(*con*-Au@Ag)@PANI, citrate-stabilized Au NPs (d_{av} = 19 nm) were added to a solution containing aniline and a surfactant, sodium dodecyl sulfate (SDS); $AgNO_3$ was then introduced to oxidize the aniline and initiate the surface-templated polymerization (Figure 1a).[11] The solution was mixed and then incubated at room temperature for 24 h. Its color turned from red to brown, indicating that the formation of Ag altered the plasmon resonance of the original Au NPs. The resulting NPs were then isolated by centrifugation to remove the excess reactants. Transmission electron microscopy (TEM) images showed that all of the observed NPs were uniform in size with identical structure (Figure 1b): each core was a nearly concentric Au@Ag NP that was partially encapsulated by a polymer shell. A typical image of the Au@Ag core is shown in Figure 1c, where the embedded Au seed is clearly visible because of the Au/Ag contrast under TEM. The average diameter of the metallic cores increased from the original 19 ± 1.6 nm to 24 ± 2.0 nm after the reaction. The thin Ag shells

[†] Division of Chemistry and Biological Chemistry, Nanyang Technological University.
[‡] Northeast Normal University.
[§] School of Materials Science and Engineering, Nanyang Technological University.

did not show clear facets at this stage. In the UV−vis spectra, the original Au absorption at 520 nm was blue-shifted to 483 nm and a new Ag absorption peak appeared at 410 nm,[11] supporting the formation of Au@Ag cores. When the NPs were dried in the presence of a 0.26 mM $(NH_4)_6Mo_7O_{24}$ stain solution, the *ecc*-(*con*-Au@Ag)@PANI NPs spontaneously assembled into dimers and small clusters with the metallic cores facing one another (Figure 1d). This specificity demonstrated the different surface functionalities of the Janus NPs. When stabilized by SDS, the PANI shell is less prone to aggregation than the Au@Ag core. While TEM was not an ideal method for exploring the existence of very thin PANI shells on the "exposed" metal surface, the "exposed" surface at least behaved differently than the PANI-coated surface in terms of NP assembly and Ag growth (see below).

Despite the complex nanostructure, the synthesis was extremely simple and readily scalable. All one has to do is mix the ingredients in the right ratio at room temperature and then wait for some time. Scaling up the reaction to 40 mL (Figure 1c inset) gave the same Janus NPs with uniform structure and narrow size distribution.[11] The purified NPs were stable in SDS solutions for weeks without aggregation unless a salt was added.

In this system, the Au seeds played an important role in controlling the size uniformity of the *ecc*-(*con*-Au@Ag)@PANI NPs. In their absence, irregular *ecc*-Ag@PANI formed[11] as a result of continuous homogeneous nucleation (i.e., formation of free Ag seeds) and the different growth times experienced by the seeds. Introducing uniform prefabricated Au seeds led to same growth time for all of the NPs and thus a more uniform size distribution.

Various types of seeds, such as Ag nanocubes and Au nanorods (NRs), can be used for this synthesis. The resulting NPs appeared to be crystalline in shape with parallel facets indicating internal lattice order (Figure 2b).[11] Intriguingly, the PANI shell often grew on only one side of the Au NRs, but the Ag growth occurred in all directions, including the side coated with thick PANI shell (∼50 nm; Figure 2b). Thus, it is clear that Ag^+ ions or Ag^0 atoms were able to diffuse through the shell and be deposited on the Au surface. As a result, the Au NR seeds were only slightly off center in the cores. Since all of the side facets of the Au NRs ({110} and {100}) were not coated with PANI, it is unlikely that the polymer attachment was facet-specific. This argument is supported by the results when long Au NRs (l = 280 nm, aspect ratio = 14) were used, which led to encircling PANI shells (length = 130 ± 12 nm) on only a section of the rods (Figure 2c). The crystal facets along the same side of the Au NRs are expected to be the same, but they were not uniformly coated. Instead, the PANI shells behaved more like liquid droplets and appeared to have moved along the rods.

A notable difference between panels b and c in Figure 2 is that the shells on the short Au NRs did not extend over to the other side, whereas those on the long Au NRs encircled the rods. In emulsion systems, it is well-known that the equilibrium configuration of a three-phase system (*i*, *j*, and *k*) depends on the balance of interfacial tensions σ_{jk}, σ_{ij}, and σ_{ik}.[12] While the metallic core in our system is rigid, the PANI nanodroplet tends to minimize its total surface energy at the Ag−PANI and PANI−water interfaces. Thus, the polymer shell moved to the side of the short Au NRs to minimize the Ag−PANI interface and assumed a partially spherical shape to reduce the PANI−water interface. In contrast, the PANI droplets attached to long Au NRs have an ellipsoidal shape supported by the rods. In view of their large size, it was probably less energetically costly to encircle the narrow rods than to attach to only one side (Figure 2c inset).[3b,13]

Our investigation of the mobility of the PANI shells revealed that those on *ecc*-(*con*-Au@Ag)@PANI NPs could move to become more

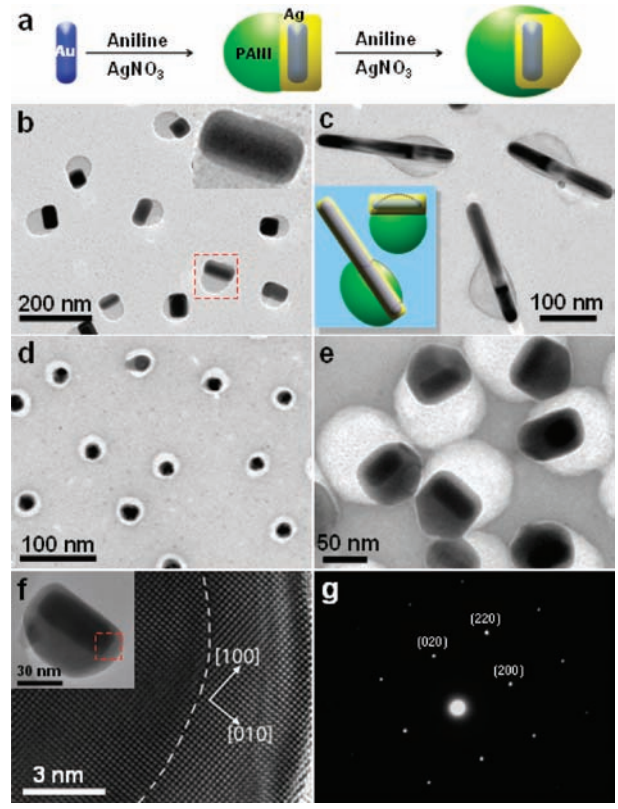

Figure 2. (a) Schematic illustration of the colloidal synthesis of Janus NPs using Au NRs as seeds. The partial polymer shells on the Au NRs were used to aid the subsequent growth of eccentric bimetallic Au@Ag cores. (b, c) TEM images of *ecc*-(Au@Ag)@PANI NPs synthesized from Au NRs with low and high aspect ratios, respectively. The inset in (c) shows schematics explaining the different configurations of the PANI shells in (b) and (c). (d) *con*-(*con*-Au@Ag)@PANI NPs obtained from a reaction at 80 °C under otherwise the same reaction conditions as for Figure 1b. (e) *ecc*-(*ecc*-Au@Ag)@PANI NPs grown from Au NRs that underwent reaction for 3 days. (f) HRTEM image of the Au−Ag interface in an *ecc*-(*ecc*-Au@Ag)@PANI NP.[11] The inset shows an overview of the whole Au@Ag core. (g) SAED pattern of an *ecc*-Au@Ag core.

eccentric when the NPs were incubated in a more concentrated SDS solution (4 mM; $[SDS]_{CMC}$ = 8 mM) overnight (Figure 1e). As a longer incubation time did not cause further movement, it appeared that equilibrium states were attained. Control samples incubated in the as-synthesized solution did not change structure. Thus, the SDS concentration was the critical factor, and this result was reproduced with eccentric PANI shells on Au NRs.[11] It is a rare case where the dynamics of core−shell structures was observed in nanoscale. The high surface density of SDS on PANI reduced $\sigma_{PANI-water}$, which in turn affected the balance of the interactions. Upon SDS treatment, some of the PANI shells on the NRs were completely detached, probably because the reduction in $\sigma_{PANI-water}$ led to the condition that $\sigma_{Ag-PANI} > \sigma_{PANI-water} + \sigma_{Ag-water}$, which transformed the equilibrium configuration whereby Au@Ag cores cannot be engulfed in PANI.[12]

A number of factors can affect the mobility of PANI shells, leading to kinetically trapped configurations. The (Au@Ag)@PANI synthesized at 80 °C under otherwise the same conditions gave fully encapsulated, concentric NPs (Figure 2d). We speculate that this result may be related to the higher degree of aniline polymerization or cross-linking that occurred at higher temperature.[5a] Both 80 °C incubation and $(NH_4)_2S_2O_8$ treatment can render the PANI shells of prefabricated *ecc*-(*con*-Au@Ag)@PANI NPs immobile in 4 mM SDS solution,[11] supporting this argument. Previously, *con*-(*con*-Au@Ag)@PPy NPs were synthesized at room temperature

using $AgNO_3$ as the oxidant for pyrrole,[10a] and *con*-Au@PANI NPs were fabricated when $(NH_4)_2S_2O_8$ was used to oxidize aniline.[10b,11] In view of the similarity between the systems, it is possible that the immobility of the polymer shell was responsible for the concentric core−shell structures.

Nevertheless, the reproducible formation of anisotropic polymer shells in this current system provided an interesting opportunity to reduce the symmetry of the bimetallic cores. Although Ag^+/Ag^0 can diffuse through the PANI shell, the rate should be lower than the rate of direct deposition on the exposed metal surface. The key is to promote uneven Ag deposition without compromising the size uniformity of the cores. Since the newly formed Ag blocks were often single-crystalline, the use of polycrystalline Au NPs as seeds led to irregular NPs upon extensive Ag growth.[11] On the other hand, concentrated $AgNO_3$ gave anisotropic but highly inconsistent Au@Ag cores. A strategy that worked was to use single-crystalline Au NRs as seeds and employ a low concentration of excess $AgNO_3$ to oxidize aniline over a prolonged period of time (3 days). TEM images of the resulting NPs showed a triple-layer structure with eccentric cores (Figure 2e). The embedded Au NRs in the metallic cores were visible under TEM and could be identified on the basis of their size and shape. Energy dispersive X-ray (EDX) line-scan analysis of the bimetallic cores confirmed the chemical composition therein.[11] In comparison with the *ecc*-(*con*-Au@Ag)@PANI NPs in Figure 2b, Ag growth did occur underneath the thick PANI shell but was significantly less than the growth on the exposed side opposite the PANI shell, where faster Ag deposition had led to wedged tips of greater Ag volume. Hence, the presence of the PANI shell affected the rate of Ag growth. During the initial stage of reaction, the newly formed thin PANI shells probably did not cause significant anisotropic growth (Figures 1b and 2b), but with the accumulation of PANI, the Ag growth at a later stage was greatly affected.

However, it appeared that the PANI shell was not the only determining factor for controlling the Ag growth. The bases of the Ag wedges were flat and parallel to the sides of the Au NRs (Figure 2e), despite the different diffusion length from the solution to the various points along the base. Thus, the crystal facets of Ag probably also played an important role. The wedged shape was likely a result of the stable Ag(111) facets in solution in comparison with the Ag(110) or Ag(100) facets in PANI. The crystal structure of the *ecc*-Au@Ag cores was studied by high-resolution TEM (HRTEM, Figure 2f). While it was difficult to confirm the lattice fringe of Au because of the thick Ag coating, the lattice fringe of the peripheral Ag block was found to align with the lattice of the Au NR on the basis of the rod orientation. The selected-area electron diffraction (SAED) pattern of an overall *ecc*-Au@Ag core (Figure 2g) showed a simple superimposed diffraction pattern, supporting the hypothesis that the Au and Ag components have matching lattices. Thus, we assigned the Ag facets according to those of the Au NRs.

Despite the complex structures of the *ecc*-(*con*-Au@Ag)@PANI and *ecc*-(*ecc*-Au@Ag)@PANI NPs obtained from Au NR seeds, the UV−vis spectra of these NPs were, unfortunately, not extraordinary.[11] With the thin Ag layer on the *con*-Au@Ag cores, the transverse and longitudinal plasmon resonance absorption peaks of the Au NRs were blue-shifted from 517 to 504 nm and from 634 to 563 nm, respectively, accompanied by the formation of a shoulder peak of Ag at 421 nm. For the *ecc*-(*ecc*-Au@Ag)@PANI NPs, the thick Ag layer (>10 nm) masked the Au absorption and led to a major absorption peak at 514 nm with a weak shoulder at 403 nm.

Controlling crystal facets is arguably the most facile and versatile approach for fine-tuning the shape of nanocrystals, and seeded epitaxial growth provides additional abilities to control the internal structures while achieving overall size uniformity. Our observations that Ag could epitaxially grow on Au seeds in the presence of polyaniline shells and that the growth could be modulated gave rise to interesting opportunities. We have demonstrated here the feasibility of using eccentric polymer shells to break the symmetry of bimetallic Au@Ag nanoparticles. Combined with the epitaxial growth, this approach can lead to rational control of complex nanocrystals of unusual shapes, which are critical for exploring physical properties and for fabricating nanocomponents for advanced nanoassembly. Our facile colloidal synthesis ensures a sufficient quantity of complex nanoparticles for these future developments.

Acknowledgment. The authors thank the Ministry of Education, Singapore, for financial support (RG 52/07 and ARC 27/07).

Supporting Information Available: Synthesis and characterization details and supporting figures. This material is available free of charge via the Internet at http://pubs.acs.org.

References

(1) (a) Xia, Y.; Yang, P.; Sun, Y.; Wu, Y.; Mayers, B.; Gates, B.; Yin, Y.; Kim, F.; Yan, H. *Adv. Mater.* **2003**, *15*, 353. (b) Murphy, C. J.; Sau, T. K.; Gole, A. M.; Orendorff, C. J.; Gao, J.; Gou, L.; Hunyadi, S. E.; Li, T. *J. Phys. Chem. B* **2005**, *109*, 13857. (c) Tao, A. R.; Habas, S.; Yang, P. *Small* **2008**, *4*, 310. (d) Wang, X.; Li, G.; Chen, T.; Yang, M.; Zhang, Z.; Wu, T.; Chen, H. *Nano Lett.* **2008**, *8*, 2643. (e) Chen, G.; Wang, Y.; Tan, L. H.; Yang, M.; Tan, L. S.; Chen, Y.; Chen, H. *J. Am. Chem. Soc.* **2009**, *131*, 4218. (f) Chen, G.; Wang, Y.; Yang, M.; Xu, J.; Goh, S. J.; Pan, M.; Chen, H. *J. Am. Chem. Soc.* **2010**, *132*, 3644.

(2) (a) DeVries, G. A.; Brunnbauer, M.; Hu, Y.; Jackson, A. M.; Long, B.; Neltner, B. T.; Uzun, O.; Wunsch, B. H.; Stellacci, F. *Science* **2007**, *315*, 358. (b) Nakata, K.; Hu, Y.; Uzun, O.; Bakr, O.; Stellacci, F. *Adv. Mater.* **2008**, *20*, 4294.

(3) (a) Love, J. C.; Gates, B. D.; Wolfe, D. B.; Paul, K. E.; Whitesides, G. M. *Nano Lett.* **2002**, *2*, 891. (b) Mock, E. B.; De Bruyn, H.; Hawkett, B. S.; Gilbert, R. G.; Zukoski, C. F. *Langmuir* **2006**, *22*, 4037. (c) Nie, Z.; Li, W.; Seo, M.; Xu, S.; Kumacheva, E. *J. Am. Chem. Soc.* **2006**, *128*, 9408. (d) Yu, H. K.; Mao, Z.; Wang, D. *J. Am. Chem. Soc.* **2009**, *131*, 6366.

(4) (a) Paunov, V. N.; Cayre, O. J. *Adv. Mater.* **2004**, *16*, 788. (b) Xu, X.; Rosi, N. L.; Wang, Y.; Huo, F.; Mirkin, C. A. *J. Am. Chem. Soc.* **2006**, *128*, 9286. (c) Huo, F.; Lytton-Jean, A. K. R.; Mirkin, C. A. *Adv. Mater.* **2006**, *18*, 2304.

(5) (a) Ge, J.; Hu, Y.; Zhang, T.; Yin, Y. *J. Am. Chem. Soc.* **2007**, *129*, 8974. (b) Guo, S.-R.; Gong, J.-Y.; Jiang, P.; Wu, M.; Lu, Y.; Yu, S.-H. *Adv. Funct. Mater.* **2008**, *18*, 872. (c) Chen, T.; Yang, M.; Wang, X.; Tan, L. H.; Chen, H. *J. Am. Chem. Soc.* **2008**, *130*, 11858. (d) Ohnuma, A.; Cho, E. C.; Camargo, P. H. C.; Au, L.; Ohtani, B.; Xia, Y. *J. Am. Chem. Soc.* **2009**, *131*, 1352. (e) Tan, L. H.; Xing, S.; Chen, T.; Chen, G.; Huang, X.; Zhang, H.; Chen, H. *ACS Nano* **2009**, *3*, 3469.

(6) (a) Gu, H.; Zheng, R.; Zhang, X.; Xu, B. *J. Am. Chem. Soc.* **2004**, *126*, 5664. (b) Yu, H.; Chen, M.; Rice, P. M.; Wang, S. X.; White, R. L.; Sun, S. *Nano Lett.* **2005**, *5*, 379. (c) Glaser, N.; Adams, D. J.; Böker, A.; Krausch, G. *Langmuir* **2006**, *22*, 5227. (d) Yang, J.; Elim, H. I.; Zhang, Q.; Lee, J. Y.; Ji, W. *J. Am. Chem. Soc.* **2006**, *128*, 11921. (e) Yang, J.; Peng, J.; Zhang, Q.; Peng, F.; Wang, H.; Yu, H. *Angew. Chem., Int. Ed.* **2009**, *48*, 3991.

(7) (a) Lee, Y. W.; Kim, M.; Kim, Z. H.; Han, S. W. *J. Am. Chem. Soc.* **2009**, *131*, 17036. (b) Lim, B.; Jiang, M.; Camargo, P. H. C.; Cho, E. C.; Tao, J.; Lu, X.; Zhu, Y.; Xia, Y. *Science* **2009**, *324*, 1302. (c) Cho, E. C.; Camargo, P. H. C.; Xia, Y. *Adv. Mater.* **2010**, *22*, 744.

(8) (a) Habas, S. E.; Lee, H.; Radmilovic, V.; Somorjai, G. A.; Yang, P. *Nat. Mater.* **2007**, *6*, 692. (b) Fan, F.-R.; Liu, D.-Y.; Wu, Y.-F.; Duan, S.; Xie, Z.-X.; Jiang, Z.-Y.; Tian, Z.-Q. *J. Am. Chem. Soc.* **2008**, *130*, 6949. (c) Lim, B.; Wang, J.; Camargo, P. H. C.; Jiang, M.; Kim, M. J.; Xia, Y. *Nano Lett.* **2008**, *8*, 2535. (d) Park, K.; Vaia, R. A. *Adv. Mater.* **2008**, *20*, 3882. (e) Lim, B.; Kobayashi, H.; Yu, T.; Wang, J.; Kim, M. J.; Li, Z.-Y.; Rycenga, M.; Xia, Y. *J. Am. Chem. Soc.* **2010**, *132*, 2506.

(9) (a) Camargo, P. H. C.; Xiong, Y.; Ji, L.; Zuo, J. M.; Xia, Y. *J. Am. Chem. Soc.* **2007**, *129*, 15452. (b) Xiang, Y.; Wu, X.; Liu, D.; Li, Z.; Chu, W.; Feng, L.; Zhang, K.; Zhou, W.; Xie, S. *Langmuir* **2008**, *24*, 3465. (c) Xiang, Y.; Wu, X.; Liu, D.; Feng, L.; Zhang, K.; Chu, W.; Zhou, W.; Xie, S. *J. Phys. Chem. C* **2008**, *112*, 3203. (d) Seo, D.; Yoo, C. I.; Jung, J.; Song, H. *J. Am. Chem. Soc.* **2008**, *130*, 2940.

(10) (a) Xing, S.; Tan, L. H.; Chen, T.; Yang, Y.; Chen, H. *Chem. Commun.* **2009**, 1653. (b) Xing, S.; Tan, L. H.; Yang, M.; Pan, M.; Lv, Y.; Tang, Q.; Yang, Y.; Chen, H. *J. Mater. Chem.* **2009**, *19*, 3286.

(11) See the Supporting Information for details and larger images.

(12) Torza, S.; Mason, S. G. *J. Colloid Interface Sci.* **1970**, *33*, 67.

(13) Casavola, M.; Buonsanti, R.; Caputo, G.; Cozzoli, P. D. *Eur. J. Inorg. Chem.* **2008**, 837.

JA102591Z